NEUROSCIENCE

A switch in G protein coupling for type 1 corticotropin-releasing factor receptors promotes excitability in epileptic brains

Chakravarthi Narla,[1,2] Tanner Scidmore,[1,2] Jaymin Jeong,[1,3] Michelle Everest,[1] Peter Chidiac,[2,4] Michael O. Poulter[1,2,3]*

Anxiety and stress increase the frequency of epileptic seizures. These behavioral states induce the secretion of corticotropin-releasing factor (CRF), a 40–amino acid neuropeptide neurotransmitter that coordinates many behavioral responses to stress in the central nervous system. In the piriform cortex, which is one of the most seizurogenic regions of the brain, CRF normally dampens excitability. By contrast, CRF increased the excitability of the piriform cortex in rats subjected to kindling, a model of temporal lobe epilepsy. In nonkindled rats, CRF activates its receptor, a G protein (heterotrimeric guanosine triphosphate–binding protein)–coupled receptor, and signals through a $G\alpha_{q/11}$-mediated pathway. After seizure induction, CRF signaling occurred through a pathway involving $G\alpha_s$. This change in signaling was associated with reduced abundance of regulator of G protein signaling protein type 2 (RGS2), which has been reported to inhibit $G\alpha_s$-dependent signaling. RGS2 knockout mice responded to CRF in a similar manner as epileptic rats. These observations indicate that seizures produce changes in neuronal signaling that can increase seizure occurrence by converting a beneficial stress response into an epileptic trigger.

INTRODUCTION

Aversive emotional experiences increase both the frequency and the severity of seizures in humans and in animal models (*1*, *2*). Epileptic patients are also more vulnerable to suicide, anxiety attacks, and depression than healthy individuals (*3*, *4*). Negative emotions such as worry and fear resulting from stress and depression affect neuronal activity within many brain regions, including limbic structures, such as amygdala, hippocampus, and piriform cortex; these brain regions also support epileptiform activity. The epileptic brain could be more susceptible to otherwise normal stress responses or, alternatively, the brain state could change the nature of the stress response so that it now promotes seizures. Several hormones and neurotransmitters are increased by anxiety and stress conditions and might therefore be involved in stress-dependent seizurogenesis. Basal concentrations of stress hormones are increased in epileptic patients compared to healthy individuals. For instance, increased seizure frequency is observed with increased concentrations of cortisol in epilepsy patients (*5*). The polypeptide hormone corticotropin-releasing factor (CRF), which also acts as a neurotransmitter, might also serve to increase seizure frequency and has been linked with various psychological disorders (*6*). The presence of CRF immunoreactive cell bodies in the paraventricular nucleus (PVN) links CRF to the endocrine stress axis, and the dense distribution of CRF immunoreactivity in the dorsal raphe nucleus and locus coeruleus implicates CRF in the modulation of monoaminergic pathways. Individuals with major depressive disorder may have hyperactive hypothalamo-pituitary-adrenal axis functioning, including CRF hypersecretion and increased CRF mRNA in PVN (*7*).

In other portions of the central nervous system, CRF is released from axons arising from cells of the central amygdala and interneurons (*8*–*10*). It acts on type 1 CRF receptors ($CRFR_1$) with high affinity and with low affinity on $CRFR_2$, both of which are G protein [heterotrimeric guanosine triphosphate (GTP)–binding protein]–coupled receptors (GPCRs). We have shown that in the piriform cortex, CRF acting through $CRFR_1$ dampens excitation of the piriform cortex circuitry (*11*), whereas it usually increases excitability in other brain regions (*8*). This activity is likely mediated through activation of $G\alpha_{q/11}$ signaling path because protein kinase C (PKC) activation and antagonism either mimic or block the activity of CRF, respectively.

Because epileptic seizures are exacerbated by anxiety and stress, we decided to test the hypothesis that the effect of CRF could depend on the underlying condition of the brain or its disease state. We used the kindling model of epilepsy, which mimics many aspects of temporal lobe epilepsy in humans (*12*). In contrast to the normal brain state, we found that CRF augmented the principle cell excitation in kindled piriform cortex. This alteration in function appears to be due to a change in the signaling pathway activated by the $CRFR_1$ receptor, which occurs through the down-regulation of a regulator of G protein signaling protein type 2 (RGS2).

RESULTS

Upon activation of the piriform cortex by stimulation of the lateral olfactory tract (LOT) in nonkindled rats, CRF reduced the excitation of layer II dorsal endopiriform nucleus (DEn) neurons and the inhibition of layer III inhibitory interneurons, resulting in reduced disinhibition of layer II neurons (Fig. 1, A to D), as indicated by voltage-sensitive dye imaging (VSDI) (movies S1 and S2). By contrast, in kindled rats, CRF increased layer II and DEn activity, whereas in layer III, it further decreased the neuronal activity, enhancing disinhibition (Fig. 1, E to H, and movies S3 and S4). Thus, after kindling, CRF enhanced circuit activation, an effect opposite to that in sham-operated control rats. We hypothesized that this switch in activity could be due to changes in the relative abundance of CRFRs (type 1 compared to type 2) or in CRF abundance (an increase so that endogenous release might activate $CRFR_2$). Immunohistochemical analyses revealed that $CRFR_1$ protein abundance was unaltered in all of the layers of the piriform cortex

[1]Molecular Medicine Research Group, Robarts Research Institute, Schulich School of Medicine, University of Western Ontario, London, Ontario N6A 5K8, Canada. [2]Department of Physiology and Pharmacology, Schulich School of Medicine, University of Western Ontario, London, Ontario N6A 3K7, Canada. [3]Graduate Program in Neuroscience, Schulich School of Medicine, University of Western Ontario, London, Ontario N6A 5K8, Canada. [4]Department of Biology, Schulich School of Medicine, University of Western Ontario, London, Ontario N6A 3K7, Canada.
*Corresponding author. Email: mpoulter@robarts.ca

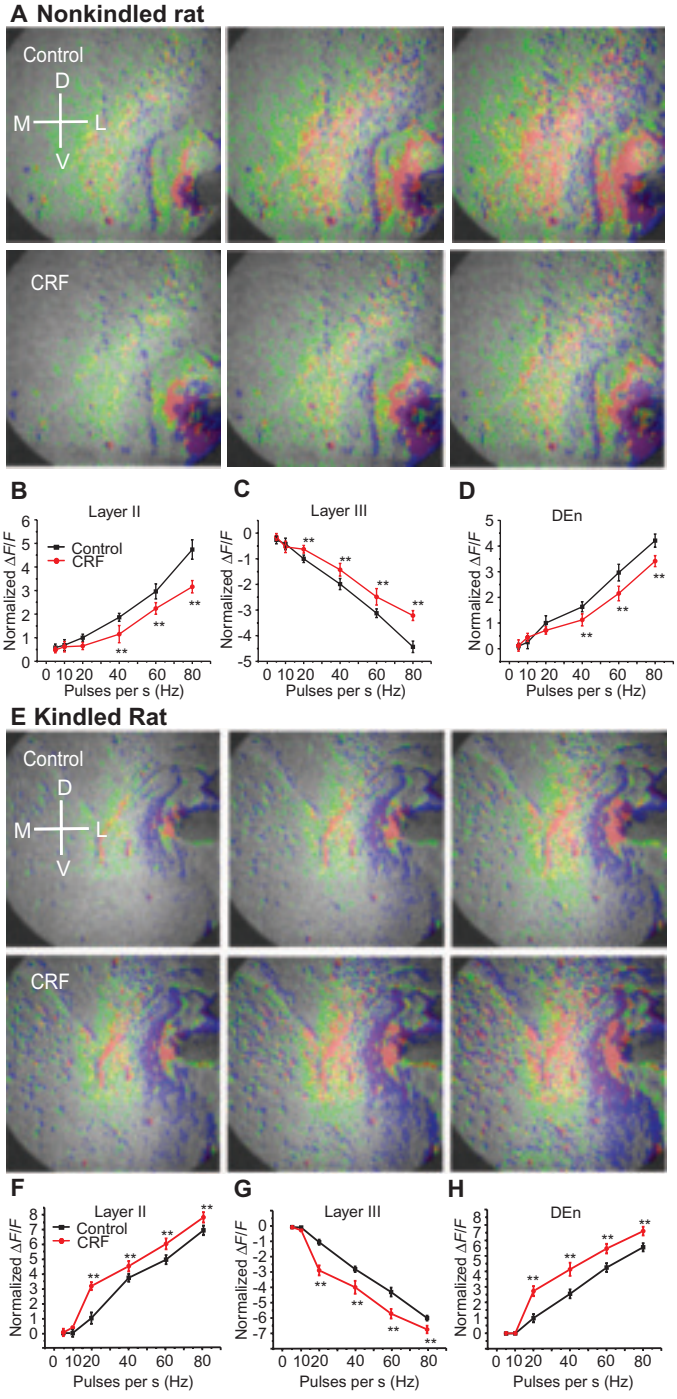

Fig. 1. Activation of $CRFR_1$ by CRF dampened piriform cortex circuitry in normal rats but potentiated it in kindled rats. (A) Representative images showing activation of piriform cortex from nonkindled rats without (top) or with (bottom) CRF perfusion before recording. Each image in the bottom row was taken at the same time interval as that of its corresponding image in the top row. (B to D) Quantification of $CRFR_1$ activation shows that the activity of layer II pyramidal cells and interneurons of DEn is increased, whereas that of layer III interneurons is decreased in nonkindled animals over the range of stimulation frequencies used to activate the circuit. $^{**}P < 0.01$. $n = 7$ slices from six rats. (E) Representative images showing activation of layers of piriform cortical slices from kindled rats without (top) or with (bottom) CRF perfusion before recording. (F to H) Quantification of $CRFR_1$ activation shows that the activity of layer II pyramidal cells and interneurons of DEn is decreased, whereas that of layer III interneurons is increased in nonkindled animals over the range of stimulation frequencies used in piriform cortical slices from kindled rats to activate the circuit. $^{**}P < 0.01$. Kindled $n = 13$ slices from nine rats. Arrows in (A) and (E) indicate orientation of slice. D, dorsal; V, ventral; M, medial; L, lateral. Red, highest $\Delta F/F$; orange, yellow, and green, medium $\Delta F/F$; blue, low $\Delta F/F$.

(fig. S1A) and that $CRFR_2$ abundance was low and unchanged as well (fig. S1B). The distribution and abundance of the CRF peptide were also unchanged (fig. S1C). As in normal controls, CRF acted through the activation of $CRFR_1$ because antalarmin, a $CRFR_1$ antagonist, blocked the effects of CRF in kindled rats (Fig. 2). The median inhibitory concentration (IC_{50}) for antalarmin increased to about 200 nM, which is in contrast to the 100 nM that has been previously reported by our group in nonkindled rats (*11*).

Because there was no change in CRFR or CRF peptide abundance and the effects were mediated through the same receptors, we next investigated the signaling pathways involved in CRF responses. We have previously reported that in nonkindled animals, $CRFR_1$ signals by activating PKC through $G\alpha_{q/11}$ (*11*). $G\alpha_{q/11}$-activated phospholipase C (PLC) hydrolyzes phosphatidylinositol 4,5-bisphosphate (PIP_2) to diacylglycerol (DG) and inositol 1,4,5-trisphosphate (IP_3). DG, a second messenger, activates PKC and facilitates further signaling cascades. Here, we showed that $CRFR_1$ signaled through the activation of a $G\alpha_s$-mediated pathway. We found that forskolin, an activator of adenylyl cyclase that mimics the effect of activated $G\alpha_s$, mimicked CRF responses, and this was antagonized by the protein kinase A (PKA) inhibitor H-89 (Fig. 3A). We also showed that H-89 blocked the effects of CRF (Fig. 3B). The application of the PKC inhibitor bisindolylmaleimide (BIS) did not block the effects of CRF (Fig. 3C), contrasting with our previous observations that application of BIS blocks the effects of CRF in nonkindled animals (*11*).

We first hypothesized that the change in signaling pathways after kindling could be due to changes in the relative abundance of $G\alpha_s$ and $G\alpha_{q/11}$ mRNA and protein. For example, an increase in $G\alpha_s$ abundance or a decrease in $G\alpha_{q/11}$ abundance could favor the coupling of $CRFR_1$ to $G\alpha_s$. However, $G\alpha_s$ mRNA expression decreased, and protein abundance was unchanged. The abundance of $G\alpha_{q/11}$ mRNA and protein was also unchanged (fig. S2). These observations therefore do not provide an explanation as to why the signaling was altered. We next considered the possibility that another mRNA(s) coding for protein(s) involved in intracellular signaling was altered. To assay for this, we used commercially available quantitative polymerase chain reaction (qPCR) arrays that permit the quantitation of mRNAs encoding 84 differing proteins involved in second messenger signal transduction, out of which 22 transcripts encoded proteins that were potentially downstream of GPCRs (fig. S3). We found that the expression of six transcripts was increased and that of four transcripts was decreased (fig. S3). However, none of the proteins encoded by these mRNAs were considered to be potentially involved in any kind of process that would cause the shift in the preferred signaling cascade. For example, we found that transcript abundance for PKC isoforms was increased, a result that might predict increased, rather than decreased, PKC signaling. We also considered

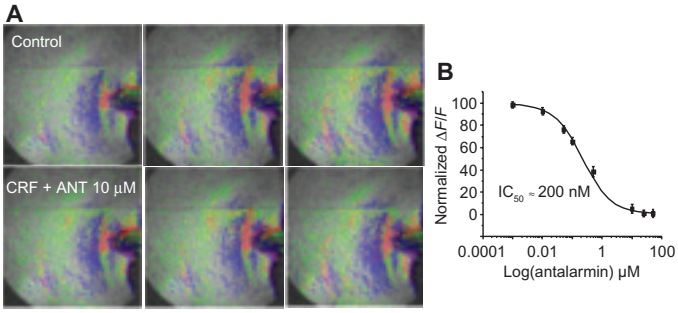

Fig. 2. CRF signals through $CRFR_1$ in kindled rat piriform cortex brain slices. (A) Representative images of the activation of the piriform cortex layers in slices at differing time points before (top) and after the application of CRF in the presence of the $CRFR_1$ antagonist antalarmin (ANT). The responses are similar in the presence of CRF and $CRFR_1$ antagonist. (B) Dose-inhibition curve for $CRFR_1$ activity in layer II over the range of concentrations of antalarmin used. $n = 9$ slices from seven rats. Red, highest $\Delta F/F$; orange, yellow, and green, medium $\Delta F/F$; blue, low $\Delta F/F$.

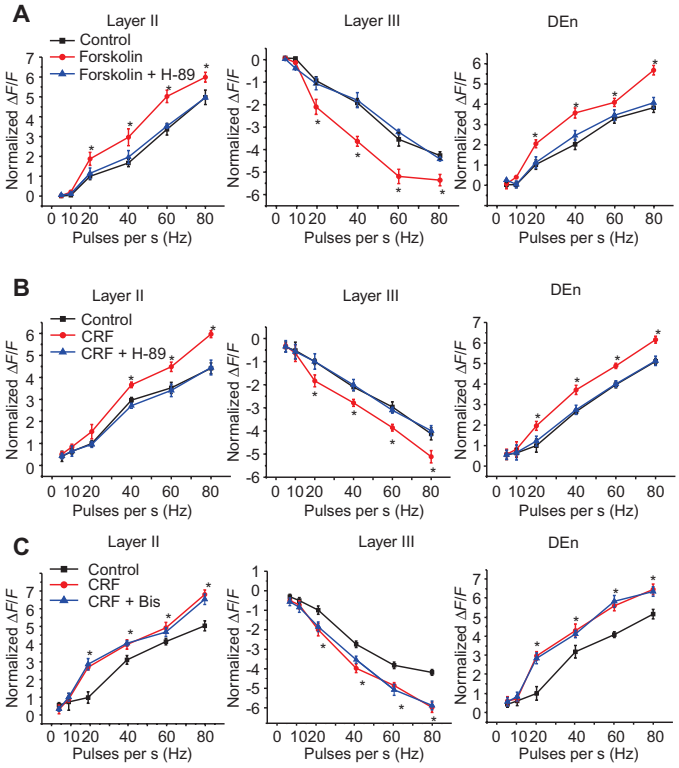

Fig. 3. CRF signals through a $G\alpha_s$-mediated signaling pathway. (A) Quantification of the effect of forskolin (an adenylyl cyclase activator) with or without subsequent administration of H-89 on $CRFR_1$ activation in piriform cortical slices from kindled animals. $^*P < 0.05$. $n = 11$ slices from nine rats per group. (B) Quantification of the effect of the PKA inhibitor H-89 on CRF-mediated activation of $CRFR_1$ in piriform cortical slices from kindled animals. $^*P < 0.05$. $n = 9$ slices from eight rats per group. (C) Quantification of the effect of the PKC antagonist BIS on CRF-mediated activation of $CRFR_1$ in piriform cortical slices from kindled animals. $^*P < 0.05$. $n = 9$ slices from seven rats per group.

the possibility that the phosphorylation states of various proteins involved in GPCR cascades could account for the change. To this end, we used a commercially available service that provides a relative assessment of the phosphorylation of 54 proteins involved in signal transduction. Again, although we found that various proteins showed changes in their phosphorylation state after kindling, none would account for a switch in signaling efficacy or preference (fig. S4).

Finally, we hypothesized that the abundance of RGS may be altered. These proteins inhibit or enhance the activity of heterotrimeric G proteins in vitro (*13–15*). Two RGS proteins, namely, RGS2 and RGS17, are abundant in the pyramidal cell layer of the piriform cortex (*13*). qPCR analysis showed that in kindled rat brain, expression of *RGS2*, but not that of *RGF17*, was decreased (Fig. 4A). In addition, RGS2 protein abundance in the layer II of the piriform cortex was reduced (Fig. 4, B and C). RGS2 has been reported to interact with and inhibit several adenylate cyclase isoforms and thus decrease cAMP (adenosine 3′,5′-monophosphate) production, thereby limiting $G\alpha_s$-mediated signaling (*16*, *17*). These observations suggest that down-regulation of RGS2 may increase $G\alpha_s$ signaling and thus may account for the switch in the $CRFR_1$ responses after kindling. To test this hypothesis, we assessed whether CRF responses in RGS2 knockout (KO) mice were similar to those observed in kindled rat brain slices. We established that CRF activity in wild-type mice was similar to that in nonkindled rats (*11*). In wild-type mouse brain slices, CRF responses were similar to those seen in rat (Fig. 5, A to D). In mice, $CRFR_1$ and $CRFR_2$ are equally abundant (unlike in rat, where $CRFR_1$ predominates); so, we verified that this response was mediated by $CRFR_1$ by showing that it was blocked by the $CRFR_1$ antagonist antalarmin (Fig. 5, E to H). In contrast, application of the $CRFR_2$ antagonist antisauvagine-30 did not block the effects of CRF (fig. S5). With the confirmation that CRF responses in wild-type mice were similar as those in nonkindled rats, we next examined CRF responses in RGS2-deficient mice. Like in kindled rats (Fig. 1E), CRF increased the excitability of the piriform cortex in RGS2 KO mice (Fig. 6, A to D). In wild-type mice, we found that the PKC antagonist BIS blocked the effects of CRF, indicating that $CRFR_1$ was likely signaled by a $G\alpha_{q/11}$-dependent pathway (Fig. 6, E to G). These observations are similar to our observations in the nonkindled rats (*11*). By contrast, in RGS2 KO mice, the PKA

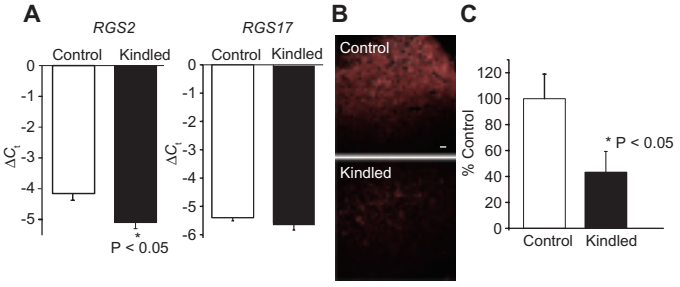

Fig. 4. RGS2 mRNA and protein abundance is decreased in kindled rats. (A) Δ cycle threshold (ΔC_t) was compared between kindled ($n = 11$) and nonkindled ($n = 9$) samples. $^*P < 0.05$. ΔC_t is the C_t (reference gene) − C_t (gene of interest). Analysis shows that *RGS2* mRNA transcripts are significantly decreased in kindled piriform cortex in comparison to control. No significant difference is observed in *RGS17* mRNA expression between nonkindled and kindled animals. (B) Representative confocal images indicating reduced RGS2 abundance in layer II after kindling. The brightest pixels three times above background have been marked in white to indicate differences in expression (scale bar, 20 mm). (C) Relative percentage of pixels that were above this cutoff ($n = 5$ slices from five control rats; $n = 4$ slices from four kindled rats; $^*P < 0.05$).

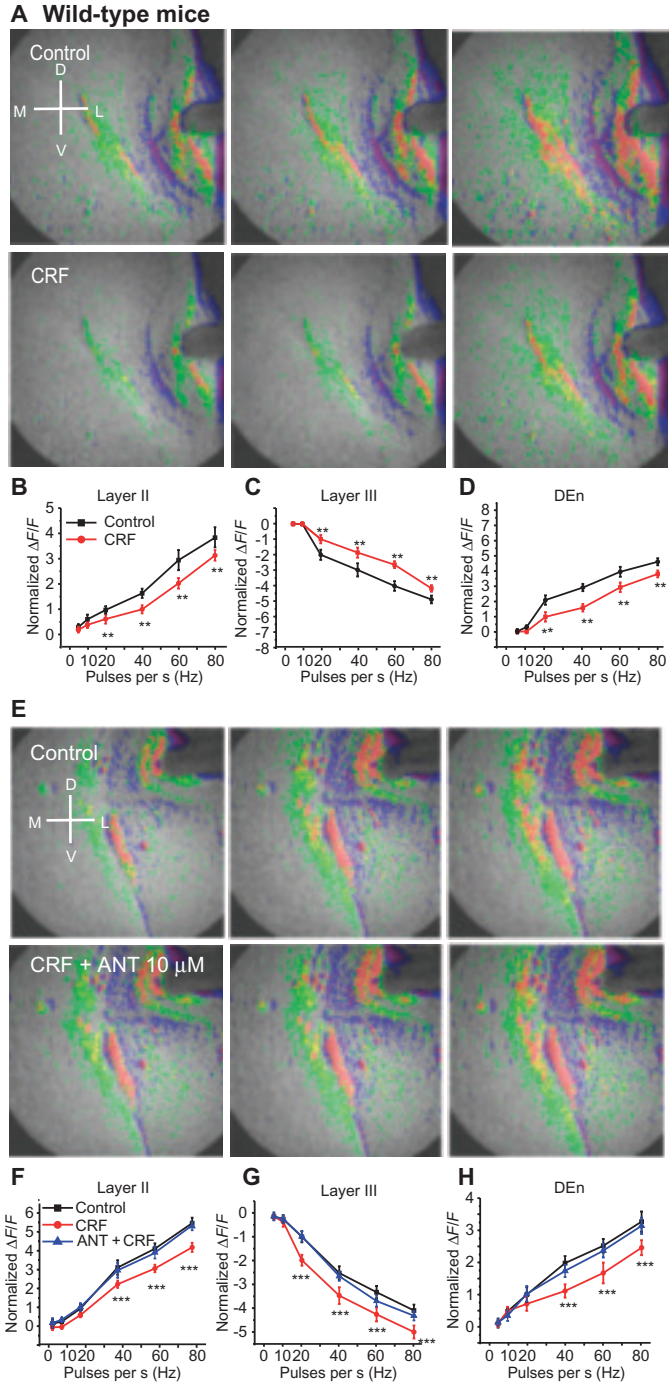

Fig. 5. Application of CRF dampened piriform cortex circuitry through $CRFR_1$ in wild-type mice. (A) Representative images of activation of layers of piriform cortex from wild-type mice without (top) or with (bottom) CRF perfusion before recording. (B to D) Quantification of CRFR1 activation shows decreased excitation in layer II and DEn and increased disinhibition of layer III interneurons in piriform cortical slices from wild-type mice over the range of stimulation frequencies used to activate the circuit. $^{**}P < 0.01$. $n = 8$ slices from six mice per treatment. (E) Representative images of activation of layers of piriform cortex from nonkindled wild-type mice without (top) or with (bottom) perfusion of CRF and antalarmin before recording. (F to H) Quantification of $CRFR_1$ activation over the range of stimulation frequencies used in piriform cortical slices from wild-type mice to activate the circuit. $^{***}P < 0.005$. $n = 6$ slices from five mice per treatment. Each image in the bottom row of (A) and (E) was taken over the same time interval as that of its corresponding image in the top row. Red, highest $\Delta F/F$; orange, yellow, and green, medium $\Delta F/F$; blue, low $\Delta F/F$.

inhibitor H-89 blocked the effects of CRF, revealing that PKA activation was essential for signaling of $CRFR_1$ (Fig. 6, H to J). We also found that PKC antagonism using BIS in RGS KO mouse and PKA antagonism in wild-type mouse using H-89 did not affect $CRFR_1$ signaling (fig. S6).

DISCUSSION

In an animal model that resembles human temporal lobe epilepsy, we showed that the stress-related neurotransmitter CRF became excitatory and potentially more seizurogenic, reversing the polarity of its activity from inhibitory to excitatory in the piriform cortex. Our observations indicate that the epileptic state was accompanied by greater susceptibility to stressor-induced excitability in a brain region that supports seizures and seizurogenesis. These findings suggest that the underlying brain pathology may be an important determinant in the exacerbation of epilepsy in response to heightened anxiety. In effect, the neurochemical alterations support seizure onset. This observation is opposite to the one where the stressor responses are otherwise "normal" (cell signaling and polarity of the response is constant), but the epileptic state makes the brain more susceptible to an otherwise physiological response. The extent to which this alteration in brain state may account for other comorbidities or susceptibilities seen with those with epilepsy (for example, depression) is not known. In addition to epilepsy, it is also possible that similar alterations may occur in individuals who have suffered a traumatic brain injury and who can experience increased frequency of anxiety- and stress-induced seizures in brain regions that have not been directly injured. Our observations therefore provide an increased impetus to consider "bystander" outcomes that may exacerbate pathophysiological neurological outcomes.

The change in the polarity of the $CRFR_1$ signaling occurs through the switch in the signaling cascade by which CRF acts. Although $CRFR_1$ was initially classified as a GPCR that activated adenylyl cyclase (*18*), CRFR activation can activate different G protein cascades (*19–21*). For example, the neuroprotective effects of CRF in the hippocampus are mediated by the activation of PKA and MAPK (mitogen-activated protein kinase) signaling pathways (*22*). Moreover, $CRFR_1$ couples to $G\alpha_{q/11}$ in BALB/c mice hippocampal neurons, whereas it couples to $G\alpha_s$ and $G\alpha_i$ in C57BL/6N mice hippocampal neurons (*19*). In cultured hippocampal neurons, CRF regulation of *N*-methyl-D-aspartate currents is mediated by PKC, which correlates with increased PLC-β3 abundance (*23*). In prefrontal cortex pyramidal neurons, CRF activates $CRFR_1$ through the activation of PKC to enhance stressor responses (*24*). As previously mentioned, we have shown that activated $CRFR_1$ suppresses piriform cortex activity through a PKC-dependent mechanism (*11*). Thus, it seems clear that depending on the region and

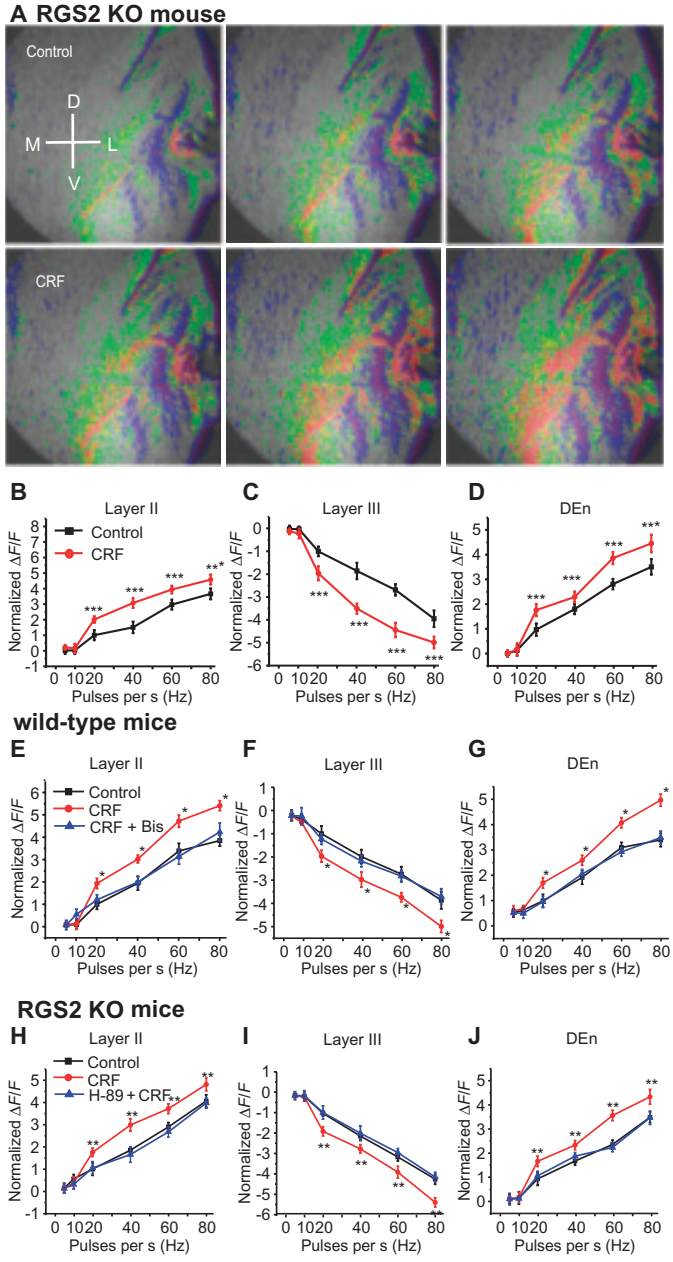

Fig. 6. Activation of $CRFR_1$ by CRF potentiated piriform cortex circuitry in RGS2 KO mice. (**A**) Representative images of activation of layers of piriform cortex from nonkindled RGS2 KO mice without (top) or with (bottom) CRF perfusion before recording. Each image in the bottom row was taken at the same time interval as that of its corresponding image in the top row. (**B** to **D**) Quantification of $CRFR_1$ activation in RGS2 KO mice shows increased excitation in layer II and DEn and increased disinhibition in layer III of piriform cortical slices from nonkindled RGS2 KO mice over the range of stimulation frequencies used to activate the circuit. ***$P < 0.005$. $n = 6$ slices from five mice per group. (**E** to **G**) Quantification of the effect of the PKC inhibitor BIS on CRF-mediated activation of $CRFR_1$ over the range of stimulation frequencies used in piriform cortical slices from nonkindled wild-type mice to activate the circuit. **$P < 0.01$. $n = 8$ slices from six mice per group. (**H** to **J**) Quantification of the effect of H-89 on CRF-mediated activation of $CRFR_1$ over the range of stimulation frequencies used in piriform cortical slices from nonkindled RGS2 KO mice to activate the circuit. **$P < 0.01$. $n = 6$ slices from five mice per group. Red, highest $\Delta F/F$; orange, yellow, and green, medium $\Delta F/F$; blue, low $\Delta F/F$.

pathological condition of the brain, $CRFR_1$ can activate distinct G proteins, resulting in activation of multiple signaling pathways. The present findings show that RGS2 protein may be an important mediator of this variation in $CRFR_1$ signaling.

GPCR signaling involves a series of complex events that lead to a conformational change of the receptor upon ligand binding and then activation of G protein by promoting exchange of GTP and GDP (guanosine diphosphate) associated with Gα. Many factors influence these events, including perceiving the extracellular signals through transducing them to heterotrimeric G proteins and to downstream effectors. RGS proteins interact with Gα subunits to attenuate GPCR-mediated signaling by accelerating Gα-GTPase (guanosine triphosphatase) activity (*13*) and/or by inhibiting G protein/effector interaction (*25*–*27*). RGS2 can inhibit $G\alpha_s$-stimulated adenylyl cyclase activity, even though it does not promote the GTPase activity of $G\alpha_s$ (*15*, *28*, *29*). RGS2 may bind directly to $G\alpha_s$ (*29*, *30*) or to adenylyl cyclase (*16*, *17*, *31*), and thus, RGS2 could produce its inhibitory effect on cAMP production by interfering with $G\alpha_s$–adenylyl cyclase coupling. Overall, these reports corroborate our findings that the presence of RGS2 in control rats decreased the production of cAMP and thus suppressed the $CRFR_1$-stimulated activity of $G\alpha_s$. However, various RGS proteins (including RGS2) have GTPase activating protein activity for $G\alpha_{q/11}$ and also function as potent inhibitors of $G\alpha_{q/11}$ signaling compared to other types of RGS proteins (*14*, *15*, *32*–*34*). Thus, it is still not clear how RGS2 is working before and after kindling, namely, how changes in RGS2 abundance might selectively favor either $G\alpha_{q/11}$- or $G\alpha_s$-mediated effects of $CRFR_1$ activation. Our findings indicated that, in the absence of RGS2 (in the KO mice) or when RGS2 abundance is low, as occurs in the kindled rat, $CRFR_1$ activation seemed to "prefer" to signal through $G\alpha_s$. Although it is easy to rationalize how a decrease in RGS2 could increase $G\alpha_s$-mediated signaling, a concomitant decrease in $G\alpha_{q/11}$-mediated signaling would not be expected. This finding recalls the decreased $G_{12/13}$ signaling effect that occurs upon a decrease in RGS5 in vascular smooth muscle (*35*), although in that case the G protein would not be considered a potential target of the RGS protein. Although RGS2 can inhibit $CRFR_1$-stimulated $G\alpha_{q/11}$ signaling, the targeting of RGS proteins to particular pathways in vivo may be governed by additional factors such as scaffolding proteins (*27*), and thus, a decrease in RGS abundance would not necessarily result in increased activation of all of its potential G protein partners.

RGS2 is present in brain regions that are implicated in the pathophysiology of anxiety and depression, such as hippocampus, amygdala, cerebral cortex, hypothalamus, and raphe nucleus of rats and mice (*15*, *36*–*38*). These regions have reciprocal connections with the piriform cortex, and pathological changes in these regions may negatively affect the physiology of the piriform cortex and perhaps seizurogenesis. Hippocampal slices from RGS2 KO mice have increased excitation in CA1 pyramidal cells, and these mice are more anxious compared to their wild-type counterparts (*39*). Moreover, a mutation in the *RGS2* gene causes anxiety in mice (*40*), and decreased RGS2 abundance is associated with depression-like behavior in mutant mice (*41*). Thus, the relationship between RGS2 abundance and behavior may depend on whether anxiety or depression is also present, which may limit the usefulness of drugs targeting RGS2.

Several studies have reported the clinical implications of RGS2 and complications associated with its polymorphisms. RGS2 has been proposed to be an important drug target in anxiety-related disorders, depression, and panic disorders in humans (*42*, *43*). Several studies have reported the pathogenetic association of single-nucleotide polymorphisms (SNPs) especially rs4606 in the *RGS2* gene and neuropsychiatric disorders. *RGS2* gene polymorphism has been associated with the development of panic disorder related to agoraphobia in 173 subjects of German descent (*38*). Furthermore, abnormalities in serotonin receptor function due to *RGS2* gene polymorphisms have been found in Japanese suicide victims (*44*). Examination of postmortem brains revealed significant differences in allele frequencies of two SNPs (SNP 2 and 3) in suicide victims compared to controls. Moreover, RGS2 immunoreactivity is greatest in the amygdala and BA9 region of the prefrontal cortex of suicide subjects compared to controls, suggesting that the increased RGS2 abundance alters GPCR intracellular signaling (*44*). In 2004 Florida hurricane victims, the C allele of rs4606 SNP of *RGS2* has been correlated with increased chances of developing generalized anxiety disorder, posttraumatic stress disorder, and ideation to commit suicide (*42*, *45*). Behavioral studies and functional magnetic resonance imaging have identified the association of the G allele of rs4606 SNP in anxiety-related phenotype and increased activation of the insular cortex, a part of limbic system, in human subjects (*46*). Genetic variation such as rs4606 SNP that leads to reduced RGS2 abundance is associated with antipsychotic-induced parkinsonism (*47*, *48*). Together, polymorphisms in *RGS2* in different brain regions are associated with various neurological disorders. More research is needed to understand the physiology and pathophysiology of RGS2 proteins and thus their clinical implications in human neurological disorders.

In summary, our observations provide a mechanism by which anxiety and stressors may exacerbate the occurrence of seizures. The epileptic state alters the function of a stress neurotransmitter that increases the excitability of a brain region that supports seizurogenesis, although it is uncertain how general this effect may be. Other brain pathophysiological states (such as stroke, repeated concussion, or traumatic brain injury) may also produce similar alterations in signaling in many GPCR responses. Thus, we will need to consider how mental disorders may be mitigated by the altered pathophysiological state of the brain.

MATERIALS AND METHODS

Procedures were performed in accordance with the guidelines of the Canadian Council of Animal Care and approved by the University of Western Ontario Council on Animal Care.

Kindling procedure

Kindling is a phenomenon in which the delivery of daily electrical impulses to the limbic region, such as the amygdala, leads to development of seizures and epilepsy. A detailed explanation of the surgical procedure for the electrode implantation and kindling procedure was described elsewhere (*49*).

Slice preparation and dye loading

Adult male Sprague-Dawley rats weighing 150 to 180 g or C57BL/6N mice weighing 20 to 25 g were used in our experiments. They were housed individually with free access to food and water under a continuous 12-hour light and dark cycle. Animals were anesthetized with a ketamine–medetomidine hydrochloride combination and then perfused through the heart with an ice-cold artificial cerebrospinal fluid (ACSF) in which sodium ions were replaced by choline ions (*49*). The ACSF used was composed of 110 mM choline chloride, 2.5 mM potassium chloride, 1.2 mM sodium dihydrogen phosphate, 25 mM sodium bicarbonate, 0.5 mM calcium chloride, 7 mM magnesium chloride, 2.4 mM sodium pyruvate, 1.3 mM ascorbate, and 20 mM dextrose (*50*). The brains were perfused to flush any blood out of the vessels and thereby prevent the iron in the blood from oxidizing and causing damage to neuronal cells. The brain was rapidly removed after perfusion, and the region containing anterior piriform cortex was carefully cut into a block to facilitate slicing by a Vibratome (slices were 400 μm thick). The slices were incubated at 37°C for 30 min and subsequently moved to a room temperature (22°C) bath for 45 min. The perfusion, slicing, and incubation procedures were carried out in choline-ACSF with a continuous supply of carbogen (95% O_2 and 5% CO_2 mixture). These slices were used for both VSDI and patch-clamp recording. For VSDI, slices were incubated in the voltage-sensitive dye Di-4-ANEPPS (D-199, Invitrogen Molecular Probes Inc.) for 35 min. The stock solution of the dye was dissolved in ethanol (22 mg/ml). On the day of the experiment, the dye incubation was prepared by mixing 60 μl of dye stock with 500 μl of fetal bovine serum, 500 μl of ACSF, and 310 μl of 10% Cremophor EL solution. The concentration of dye in the final solution was 0.1 mg/ml. After incubation, slices were washed for 8 to 10 min with ACSF and transferred to a recording chamber. The temperature of the bath was maintained at 32°C during recordings and continuously supplied with carbogen-bubbled ACSF, which was composed of 110 mM NaCl, 2.5 mM KCl, 1.2 mM NaH_2PO_4, 25 mM $NaHCO_3$, 2.0 mM $CaCl_2$, 2.0 mM $MgCl_2$, and 20 mM dextrose. The pH and osmolarity of the solutions were adjusted to 7.3 to 7.4 and 297 to 305 mOsm, respectively.

A platinum-iridium electrode (MicroProbes Inc.) with a tip diameter of 200 to 300 μm was used to stimulate the LOT of the piriform cortex. The stimulation of each slice was in the range of 160 to 200 μA; each square pulse was 2.0 ms in length. The electrode was connected to a stimulator (S88X Dual Output Square Pulse Stimulator, Grass Technologies, Astro-Med Inc.), which controlled the pulse frequency and train duration (*51*).

Voltage-sensitive dye imaging

Each optical recording was about 10 s in length and consisted of two phases. The first contained a recording of the background activity for 2 s followed by the application of stimulus for 1 s with a train of frequencies ranging from 5 to 80 Hz. The acquisition rate was set at 5 ms per frame. The camera saturation was set at about 50% for each recording. Optical signals were recorded by a CMOS (complementary metal oxide semiconductor) camera (MiCam Ultima Brain Vision Inc.) mounted on top of an upright microscope (fixed-stage upright microscope, BX51WI, Olympus); sections were illuminated using the light from a 100-W halogen lamp source (HLX 64625, Microlites Scientific Corp.) passed through an excitation filter (λ = 530 ± 10 nm). A long-pass emission filter (λ > 590 nm) collected the fluorescent signals. A long working distance objective was used in the experiments [XLFluor 4X, NA (numerical aperture) 0.28, Olympus]. The movies were analyzed using the Brain Vision Analyzer software. A detailed explanation of the technique is described elsewhere (*51*).

qPCR analyses

Brain tissue from microdissected piriform cortex was placed in TRIzol (Invitrogen, catalog #75649) and homogenized. Extraction of RNA from the homogenate was performed following the manufacturer's protocol. To assess purity of extracted RNA, a NanoDrop 1000 spectrometer was used. The RNA (2 μg) samples with appropriate purity (≥260/280 levels) were reverse-transcribed using the Invitrogen SuperScript II with oligo(dT) primers. For the PCR, 2 μl (40 ng) of complementary DNA (cDNA) was placed in duplicate in flat cap PCR strips. A master mix containing SYBR Green Fast Mix for iQ, along with Milli-Q water and the primers for the protein of interest, was prepared according to the manufacturer's instructions (Quanta Biosciences). Twenty-three microliters of master mix was then added to each PCR tube to make the total volume 25 μl. The strips were then

placed in a Bio-Rad MyIQ thermocycler for subsequent PCR and fluorescence detection. Primers were designed and purchased (IDT) for the mRNAs encoding Gα protein stimulatory (GNAS), G protein q polypeptide (GNAQ), RGS2, and RGS17. The primer sequences were as follows: *GNAS*, 5′-CTGCCTCGGCAACASTAAGAC-3′ (forward) and 5′-GCAGCTGCT-TCTCGATCTTTT-3′ (reverse); GNAQ, 5′-ATGCTACGATAGACGGCG-3′ (forward) and 5′-ATAGGAAGGGTCAGCCACAC-3′ (reverse); *RGS2*, 5′-CGGGAGAAAATGAAGCGGAC-3′ (forward) and 5′-AGTTT-TGGGCTTCCCAGGAG-3′ (reverse); and *RGS17*, 5′-CTAAGATGGCAGC-CAGTCGG-3′ (forward) and 5′-CCTGCGTGCCTTCATTTTGT-3′ (reverse). Primer efficiency was quantified using a five-point 10× dilution series of rat brain cDNA. The PCR primer sets were evaluated for efficiency at 55°C annealing temperature. Cyclophilin A (*PPIA*) (Sigma-Aldrich, catalog #1475-017 and #1475-018) was the reference gene to normalize expression (forward, 5′-CCGCTGTCTCTTTTCGCCGC-3′; reverse, 5′-CGAACTTTTGTCTGCAAACAGGCTCG-3′). Furthermore, 84 genes (fig. S3) that encode proteins involved in the rat dopamine and serotonin pathways were evaluated using RT^2 Profiler rat PCR arrays (PARN 158ZA-12, Qiagen). Equal amounts of pooled cDNA from nonkindled and kindled rat brains (five each) were used as template for their own respective plates. One plate was run for the nonkindled and kindled conditions; each well on the plate contained pooled genetic material of five individual rats. Each plate was run twice on separate occasions. The plate also contained five housekeeping genes, whose cycle thresholds were averaged and used for normalization of the data. Differences in the amount of mRNA present were evaluated through a comparison of the Δ cycle thresholds (C_t) between nonkindled and kindled brain samples. ΔC_t is the C_t (reference gene) − C_t (gene of interest). Mean ΔC_t between kindled and nonkindled rats was statistically analyzed using a Student's *t* test. Data are expressed as means ± SE of the ΔC_t values.

Phospho-site protein kinase screen

Samples of 250 mg of rat brain piriform cortex were washed three times in ice-cold phosphate-buffered saline (PBS) and then homogenized in lysis buffer as described in the Kinexus Bioinformatics protocol (www.kinexus.ca/). The tissue was sonicated four times for 10 s in an ice bath at 20% power with a Branson sonicator. The homogenate was then centrifuged at 20,000*g* for 30 min at 4°C in the Eppendorf Centrifuge 5810R. The supernatant was assayed for protein concentration using the Bradford assay (Bio-Rad). At a concentration of 1 mg/ml in SDS–polyacrylamide gel electrophoresis sample buffer, the samples were boiled for 4 min and then shipped on wet ice for the phospho-site protein kinase screen (catalog #KPSS 11.0) at Kinetworks Screening Services (Kinexus Bioinformatics Corp.). This assay consists of the analysis of 54 proteins that have a phosphorylation-dependent function in intracellular signaling. The complete list of the proteins assayed and the epitopes analyzed is provided in fig. S4, and further information can be found at www.kinexus.ca/. The assay quantitatively shows whether a protein has increased or decreased target phosphorylation.

Tissue preparation and fixation for immunohistochemistry

The following methodology has been described in detail elsewhere (*52*). The rats were anesthetized and perfused with 0.1 M PBS, followed by Lana's fixative (4% paraformaldehyde and 20% picric acid in PBS). The brain was removed from the skull, stored in Lana's fixative for 24 hours, and then placed in phosphate buffer solution with 30% sucrose for 48 hours at 4°C. The brains were then flash-frozen at −80°C and sectioned coronally (40 μm) using cryostat at −15°C. The sections were stored in cryoprotectant solution at −20°C.

Immunostaining

Sections were washed with PBS with 0.2% Triton X-100 three times for 5 min and blocked with 10% donkey serum and 10% goat serum in PBS with 0.025% Triton X-100 and 1% bovine serum albumin (BSA) for 1 hour. The primary antibodies were diluted in PBS with 1% BSA and 0.025% Triton X-100. The sections were labeled with a single primary antibody and incubated for 24 hours at 4°C. The primary antibodies used were anti-rabbit CRF (Abcam, ab11133, 1:250), anti-rabbit $CRFR_1$ (Abcam, ab150561, 1:250), and anti-rabbit $CRFR_2$ (Abcam, ab75168, 1:1000). The sections were then washed two times with PBS with 0.2% Triton X-100 for 5 min and incubated with a secondary antibody for 1 hour at room temperature. The secondary antibody used was Alexa Fluor 488 goat anti-rabbit immunoglobulin G (IgG) (Molecular Probes, A-11034) diluted in PBS with 1% BSA and 0.025% Triton X-100 and was diluted 1:1000 for CRF and CRFR2 and 1:2000 for $CRFR_1$. Sections were then washed three times with PBS with 0.2% Triton X-100 for 10 min and incubated in 1% Sudan Black B (Sigma-Aldrich, S2380) in 70% ethanol for 5 min. Sections were rinsed twice with 70% ethanol for 1 min followed by two 5-min washes with PBS. Sections were mounted on glass slides with glass coverslips using ProLong Gold Antifade Reagent with DAPI (4′,6-diamidino-2-phenylindole) mounting medium (Molecular Probes, P36935). Primary antibodies used were rabbit anti–G protein alpha S (Abcam, ab83735, 1:500) and rabbit anti-GNAQ (Abcam, ab75823, 1:250). The secondary antibody used was Alexa Fluor 488 goat anti-rabbit IgG (Molecular Probes, A-11034) diluted in PBS with 1% BSA and 0.02% Triton X-100 at a ratio of 1:1000. Primary antibody anti-RGS2 was used at 1:500 (Sigma-Aldrich, GW22245F) with secondary antibody Cy3 anti-chicken IgY at 1:500 (Cedarlane, 703-166-155).

Image acquisition and analysis

Confocal images were obtained using an Olympus IX51 inverted microscope using either a 60× oil immersion objective (NA, 1.4) or, for large field of viewing, a 20× objective (NA, 0.8) on a PerkinElmer UltraVIEW spinning disc confocal unit. The microscope was equipped with a Hamamatsu Orca-ER CCD (charge-coupled device) camera (1344 × 1024 pixels). All images were acquired using the Volocity software (version 4.2.1, Improvision). A stack of 10 images with 0.2-μm spacing in the *z* plane was taken. RGS2 images (Fig. 4) were acquired using a Zeiss LSM 510 Meta confocal microscope with a 40× (NA, 1.2) objective. For Fig. 4, the intensity of immunoreactivity is indicated by adding a channel (colored in white) that contains only pixels three times above background. For the semiquantitative analysis in Fig. 4C, we averaged the total amount of pixels in the field above this background value for comparison.

Statistical analysis

All statistical evaluations were done using the StatView software. Two-way analyses of variance (ANOVAs) were conducted to compare the neuronal responses after the application of BIS, PMA (phorbol 12-myristate 13-acetate), H-89, and forskolin in the piriform cortex layers in response to LOT stimulation. For CRF responses in the presence of BIS, PMA, forskolin, and H-89, a repeated-measures ANOVA was used in which responses of CRF in the absence of drugs served as the within-group measure. The pixel/voxel counts were analyzed using *t* test. Follow-up comparisons were conducted using Fisher's protected least significance difference test to maintain *P* at 0.05.

SUPPLEMENTARY MATERIALS

www.sciencesignaling.org/cgi/content/full/9/432/ra60/DC1

Fig. S1. No changes in $CRFR_1$, $CRFR_2$, or CRF immunoreactivity in the layers of the piriform cortex.

Fig. S2. The expression of the mRNAs encoding $G\alpha_s$ and $G\alpha_{q/11}$ is unchanged after kindling.

Fig. S3. qPCR analysis of mRNAs encoding proteins involved in GPCR signaling.
Fig. S4. Kindling-induced changes in the phosphorylation of signaling proteins.
Fig. S5. $CRFR_2$ antagonism did not block the effects of CRF.
Fig. S6. PKC or PKA antagonism did not affect $CRFR_1$ activation in wild-type and RGS2 KO mouse, respectively.
Movie S1. Excitation and disinhibition in the layers of nonkindled rat piriform cortex imaged through VSDI.
Movie S2. Change in the excitation and disinhibition in the layers of nonkindled rat piriform cortex after CRF application.
Movie S3. Excitation and disinhibition in the layers of kindled rat piriform cortex imaged through VSDI.
Movie S4. Change in the excitation and disinhibition in the layers of kindled rat piriform cortex after CRF application.

REFERENCES AND NOTES

1. M. M. Frucht, M. Quigg, C. Schwaner, N. B. Fountain, Distribution of seizure precipitants among epilepsy syndromes. *Epilepsia* **41**, 1534–1539 (2000).
2. H. M. de Boer, M. Mula, J. W. Sander, The global burden and stigma of epilepsy. *Epilepsy Behav.* **12**, 540–546 (2008).
3. J. M. Hettema, J. W. Kuhn, C. A. Prescott, K. S. Kendler, The impact of generalized anxiety disorder and stressful life events on risk for major depressive episodes. *Psychol. Med.* **36**, 789–795 (2006).
4. M. Pompili, P. Girardi, A. Ruberto, R. Tatarelli, Suicide in the epilepsies: A meta-analytic investigation of 29 cohorts. *Epilepsy Behav.* **7**, 305–310 (2005).
5. C. A. Galimberti, F. Magri, F. Copello, C. Arbasino, L. Cravello, M. Casu, V. Patrone, G. Murialdo, Seizure frequency and cortisol and dehydroepiandrosterone sulfate (DHEAS) levels in women with epilepsy receiving antiepileptic drug treatment. *Epilepsia* **46**, 517–523 (2005).
6. L. Arborelius, M. J. Owens, P. M. Plotsky, C. B. Nemeroff, The role of corticotropin-releasing factor in depression and anxiety disorders. *J. Endocrinol.* **160**, 1–12 (1999).
7. F. C. Raadsheer, W. J. G. Hoogendijk, F. C. Stam, F. J. H. Tilders, D. F. Swaab, Increased numbers of corticotropin-releasing hormone expressing neurons in the hypothalamic paraventricular nucleus of depressed patients. *Neuroendocrinology* **60**, 436–444 (1994).
8. G. von Wolff, C. Avrabos, J. Stepan, W. Wurst, J. M. Deussing, F. Holsboer, M. Eder, Voltage-sensitive dye imaging demonstrates an enhancing effect of corticotropin-releasing hormone on neuronal activity propagation through the hippocampal formation. *J. Psychiatr. Res.* **45**, 256–261 (2011).
9. H. Anisman, P. Prakash, Z. Merali, M. O. Poulter, Corticotropin releasing hormone receptor alterations elicited by acute and chronic unpredictable stressor challenges in stressor-susceptible and resilient strains of mice. *Behav. Brain Res.* **181**, 180–190 (2007).
10. B. Zięba, M. Grzegorzewska, P. Brański, H. Domin, J. M. Wierońska, G. Hess, M. Śmialowska, The behavioural and electrophysiological effects of CRF in rat frontal cortex. *Neuropeptides* **42**, 513–523 (2008).
11. C. Narla, H. A. Dunn, S. S. G. Ferguson, M. O. Poulter, Suppression of piriform cortex activity in rat by corticotropin-releasing factor 1 and serotonin 2A/C receptors. *Front. Cell. Neurosci.* **9**, 200 (2015).
12. D. C. McIntyre, K. L. Gilby, Kindling as a model of human epilepsy. *Can. J. Neurol. Sci.* **36** (Suppl. 2), S33–S35 (2009).
13. E. Grafstein-Dunn, K. H. Young, M. I. Cockett, X. Z. Khawaja, Regional distribution of regulators of G-protein signaling (RGS) 1, 2, 13, 14, 16, and GAIP messenger ribonucleic acids by in situ hybridization in rat brain. *Brain Res. Mol. Brain Res.* **88**, 113–123 (2001).
14. S. P. Heximer, S. P. Srinivasa, L. S. Bernstein, J. L. Bernard, M. E. Linder, J. R. Hepler, K. J. Blumer, G protein selectivity is a determinant of RGS2 function. *J. Biol. Chem.* **274**, 34253–34259 (1999).
15. T. Ingi, A. M. Krumins, P. Chidiac, G. M. Brothers, S. Chung, B. E. Snow, C. A. Barnes, A. A. Lanahan, D. P. Siderovski, E. M. Ross, A. G. Gilman, P. F. Worley, Dynamic regulation of RGS2 suggests a novel mechanism in G-protein signaling and neuronal plasticity. *J. Neurosci.* **18**, 7178–7188 (1998).
16. A. A. Roy, A. Baragli, L. S. Bernstein, J. R. Hepler, T. E. Hébert, P. Chidiac, RGS2 interacts with Gs and adenylyl cyclase in living cells. *Cell. Signal.* **18**, 336–348 (2006).
17. S. Sinnarajah, C. W. Dessauer, D. Srikumar, J. Chen, J. Yuen, S. Yilma, J. C. Dennis, E. E. Morrison, V. Vodyanoy, J. H. Kehrl, RGS2 regulates signal transduction in olfactory neurons by attenuating activation of adenylyl cyclase III. *Nature* **409**, 1051–1055 (2001).
18. R. L. Hauger, D. E. Grigoriadis, M. F. Dallman, P. M. Plotsky, W. W. Vale, F. M. Dautzenberg, International Union of Pharmacology. XXXVI. Current status of the nomenclature for receptors for corticotropin-releasing factor and their ligands. *Pharmacol. Rev.* **55**, 21–26 (2003).
19. T. Blank, I. Nijholt, D. K. Grammatopoulos, H. S. Randeva, E. W. Hillhouse, J. Spiess, Corticotropin-releasing factor receptors couple to multiple G-proteins to activate diverse intracellular signaling pathways in mouse hippocampus: Role in neuronal excitability and associative learning. *J. Neurosci.* **23**, 700–707 (2003).
20. M. J. Wanat, F. W. Hopf, G. D. Stuber, P. E. M. Phillips, A. Bonci, Corticotropin-releasing factor increases mouse ventral tegmental area dopamine neuron firing through a protein kinase C-dependent enhancement of I_h. *J. Physiol.* **586**, 2157–2170 (2008).
21. D. Wietfeld, N. Heinrich, J. Furkert, K. Fechner, M. Beyermann, M. Bienert, H. Berger, Regulation of the coupling to different G proteins of rat corticotropin-releasing factor receptor type 1 in human embryonic kidney 293 cells. *J. Biol. Chem.* **279**, 38386–38394 (2004).
22. C. R. Elliott-Hunt, J. Kazlauskaite, G. J. C. Wilde, D. K. Grammatopoulos, E. W. Hillhouse, Potential signalling pathways underlying corticotrophin-releasing hormone-mediated neuroprotection from excitotoxicity in rat hippocampus. *J. Neurochem.* **80**, 416–425 (2002).
23. H. Sheng, Y. Zhang, J. Sun, L. Gao, B. Ma, J. Lu, X. Ni, Corticotropin-releasing hormone (CRH) depresses *N*-methyl-D-aspartate receptor-mediated current in cultured rat hippocampal neurons via CRH receptor type 1. *Endocrinology* **149**, 1389–1398 (2008).
24. H. Tan, P. Zhong, Z. Yan, Corticotropin-releasing factor and acute stress prolongs serotonergic regulation of GABA transmission in prefrontal cortical pyramidal neurons. *J. Neurosci.* **24**, 5000–5008 (2004).
25. M. L. Cunningham, G. L. Waldo, S. Hollinger, J. R. Hepler, T. K. Harden, Protein kinase C phosphorylates RGS2 and modulates its capacity for negative regulation of $G\alpha_{11}$ signaling. *J. Biol. Chem.* **276**, 5438–5444 (2001).
26. M. Abramow-Newerly, A. A. Roy, C. Nunn, P. Chidiac, RGS proteins have a signalling complex: Interactions between RGS proteins and GPCRs, effectors, and auxiliary proteins. *Cell. Signal.* **18**, 579–591 (2006).
27. P. Zhao, W. Cladman, H. H. M. Van Tol, P. Chidiac, Fine-tuning of GPCR signals by intracellular G protein modulators. *Prog. Mol. Biol. Transl. Sci.* **115**, 421–453 (2013).
28. A. A. Roy, C. Nunn, H. Ming, M.-X. Zou, J. Penninger, L. A. Kirshenbaum, S. J. Dixon, P. Chidiac, Up-regulation of endogenous RGS2 mediates cross-desensitization between G_s and G_q signaling in osteoblasts. *J. Biol. Chem.* **281**, 32684–32693 (2006).
29. A. A. Roy, K. E. Lemberg, P. Chidiac, Recruitment of RGS2 and RGS4 to the plasma membrane by G proteins and receptors reflects functional interactions. *Mol. Pharmacol.* **64**, 587–593 (2003).
30. J.-K. Ko, K.-H. Choi, I.-S. Kim, E.-K. Jung, D.-H. Park, Inducible RGS2 is a cross-talk regulator for parathyroid hormone signaling in rat osteoblast-like UMR106 cells. *Biochem. Biophys. Res. Commun.* **287**, 1025–1033 (2001).
31. S. Salim, S. Sinnarajah, J. H. Kehrl, C. W. Dessauer, Identification of RGS2 and type V adenylyl cyclase interaction sites. *J. Biol. Chem.* **278**, 15842–15849 (2003).
32. J. R. Hepler, Emerging roles for RGS proteins in cell signalling. *Trends Pharmacol. Sci.* **20**, 376–382 (1999).
33. J. H. Kehrl, Heterotrimeric G protein signaling: Roles in immune function and fine-tuning by RGS proteins. *Immunity* **8**, 1–10 (1998).
34. R. K. Sunahara, J. J. G. Tesmer, A. G. Gilman, S. R. Sprang, Crystal structure of the adenylyl cyclase activator $G_{s\alpha}$. *Science* **278**, 1943–1947 (1997).
35. C. Arnold, A. Feldner, L. Pfisterer, M. Hödebeck, K. Troidl, G. Genové, T. Wieland, M. Hecker, T. Korff, RGS5 promotes arterial growth during arteriogenesis. *EMBO Mol. Med.* **6**, 1075–1089 (2014).
36. T. Ingi, Y. Aoki, Expression of RGS2, RGS4 and RGS7 in the developing postnatal brain. *Eur. J. Neurosci.* **15**, 929–936 (2002).
37. R. R. Neubig, D. P. Siderovski, Regulators of G-protein signalling as new central nervous system drug targets. *Nat. Rev. Drug Discov.* **1**, 187–197 (2002).
38. A. Leygraf, C. Hohoff, C. Freitag, S. A. G. Willis-Owen, P. Krakowitzky, J. Fritze, P. Franke, B. Bandelow, R. Fimmers, J. Flint, J. Deckert, Rgs 2 gene polymorphisms as modulators of anxiety in humans? *J. Neural Transm.* **113**, 1921–1925 (2006).
39. A. J. Oliveira-Dos-Santos, G. Matsumoto, B. E. Snow, D. Bai, F. P. Houston, I. Q. Whishaw, S. Mariathasan, T. Sasaki, A. Wakeham, P. S. Ohashi, J. C. Roder, C. A. Barnes, D. P. Siderovski, J. M. Penninger, Regulation of T cell activation, anxiety, and male aggression by RGS2. *Proc. Natl. Acad. Sci. U.S.A.* **97**, 12272–12277 (2000).
40. B. Yalcin, S. A. G. Willis-Owen, J. Fullerton, A. Meesaq, R. M. Deacon, J. N. P. Rawlins, R. R. Copley, A. P. Morris, J. Flint, R. Mott, Genetic dissection of a behavioral quantitative trait locus shows that *Rgs2* modulates anxiety in mice. *Nat. Genet.* **36**, 1197–1202 (2004).
41. T. Lifschytz, E. C. Broner, P. Zozulinsky, A. Slonimsky, R. Eitan, L. Greenbaum, B. Lerer, Relationship between *Rgs2* gene expression level and anxiety and depression-like behaviour in a mutant mouse model: Serotonergic involvement. *Int. J. Neuropsychopharmacol.* **15**, 1307–1318 (2012).
42. A. B. Amstadter, K. C. Koenen, K. J. Ruggiero, R. Acierno, S. Galea, D. G. Kilpatrick, J. Gelernter, Variant in *RGS2* moderates posttraumatic stress symptoms following potentially traumatic event exposure. *J. Anxiety Disord.* **23**, 369–373 (2009).
43. T. Otowa, T. Shimada, Y. Kawamura, N. Sugaya, E. Yoshida, K. Inoue, S. Yasuda, X. Liu, T. Minato, M. Tochigi, T. Umekage, K. Kasai, H. Tanii, Y. Okazaki, H. Kaiya, T. Sasaki, Association of *RGS2* variants with panic disorder in a Japanese population. *Am. J. Med. Genet. B Neuropsychiatr. Genet.* **156**, 430–434 (2011).
44. H. Cui, N. Nishiguchi, E. Ivleva, M. Yanagi, M. Fukutake, H. Nushida, Y. Ueno, N. Kitamura, K. Maeda, O. Shirakawa, Association of RGS2 gene polymorphisms with suicide and increased RGS2 immunoreactivity in the postmortem brain of suicide victims. *Neuropsychopharmacology* **33**, 1537–1544 (2008).

45. A. B. Amstadter, K. C. Koenen, K. J. Ruggiero, R. Acierno, S. Galea, D. G. Kilpatrick, J. Gelernter, Variation in *RGS2* is associated with suicidal ideation in an epidemiological study of adults exposed to the 2004 Florida hurricanes. *Arch. Suicide Res.* **13**, 349–357 (2009).
46. J. W. Smoller, M. P. Paulus, J. A. Fagerness, S. Purcell, L. H. Yamaki, D. Hirshfeld-Becker, J. Biederman, J. F. Rosenbaum, J. Gelernter, M. B. Stein, Influence of RGS2 on anxiety-related temperament, personality, and brain function. *Arch. Gen. Psychiatry* **65**, 298–308 (2008).
47. L. Greenbaum, R. D. Strous, K. Kanyas, Y. Merbl, A. Horowitz, O. Karni, E. Katz, M. Kotler, T. Olender, S. N. Deshpande, D. Lancet, E. Ben-Asher, B. Lerer, Association of the RGS2 gene with extrapyramidal symptoms induced by treatment with antipsychotic medication. *Pharmacogenet. Genomics* **17**, 519–528 (2007).
48. L. Greenbaum, R. C. Smith, A. Rigbi, R. Strous, O. Teltsh, K. Kanyas, M. Korner, D. Lancet, E. Ben-Asher, B. Lerer, Further evidence for association of the *RGS2* gene with antipsychotic-induced parkinsonism: Protective role of a functional polymorphism in the 3′-untranslated region. *Pharmacogenomics J.* **9**, 103–110 (2009).
49. C. Gavrilovici, S. D'Alfonso, M. Dann, M. O. Poulter, Kindling-induced alterations in $GABA_A$ receptor-mediated inhibition and neurosteroid activity in the rat piriform cortex. *Eur. J. Neurosci.* **24**, 1373–1384 (2006).
50. D. C. McIntyre, B. Hutcheon, K. Schwabe, M. O. Poulter, Divergent $GABA_A$ receptor-mediated synaptic transmission in genetically seizure-prone and seizure-resistant rats. *J. Neurosci.* **22**, 9922–9931 (2002).
51. Z. Birjandian, C. Narla, M. O. Poulter, Gain control of γ frequency activation by a novel feed forward disinhibitory loop: Implications for normal and epileptic neural activity. *Front. Neural Circuits* **7**, 183 (2013).
52. C. Gavrilovici, E. Pollock, M. Everest, M. O. Poulter, The loss of interneuron functional diversity in the piriform cortex after induction of experimental epilepsy. *Neurobiol. Dis.* **48**, 317–328 (2012).

Acknowledgments: We would like to thank K. Nan Lee for her help with the RGS2 KO mice and H. Anisman for reviewing the statistical methods used in the article. **Funding:** This work is supported by Canadian Institutes of Health Research operating grants to M.O.P. and P.C. and Natural Sciences and Engineering Research Council discovery grant to M.O.P. C.N. is supported by the Ontario Graduate Scholarship, the Western University Graduate Research Scholarship, and Schulich School of Medicine research funding. **Author contributions:** M.O.P., P.C., and C.N. conceived the experiments. C.N. carried out animal surgeries, kindling, slicing, and the VSDI experiments. J.J., T.S., and M.E. carried out immunohistochemistry and qPCR experiments. M.O.P. and C.N. analyzed the data. M.O.P., P.C., and C.N. wrote the article. C.N. and M.O.P. prepared the figures. **Competing interests:** The authors declare that they have no competing interests.

Submitted 13 November 2015
Accepted 27 May 2016
Final Publication 14 June 2016
10.1126/scisignal.aad8676
Citation: C. Narla, T. Scidmore, J. Jeong, M. Everest, P. Chidiac, M. O. Poulter, A switch in G protein coupling for type 1 corticotropin-releasing factor receptors promotes excitability in epileptic brains. *Sci. Signal.* **9**, ra60 (2016).

Science Signaling

A switch in G protein coupling for type 1 corticotropin-releasing factor receptors promotes excitability in epileptic brains

Chakravarthi Narla, Tanner Scidmore, Jaymin Jeong, Michelle Everest, Peter Chidiac and Michael O. Poulter

Sci. Signal. **9** (432), ra60.
DOI: 10.1126/scisignal.aad8676

Why stress makes epilepsy worse

Seizures caused by uncontrolled neuronal activity easily starts in a part of the brain called the piriform cortex. Normally, the activity of the piriform cortex is suppressed by CRF, a neuropeptide that is released in response to stress. Narla *et al*. found that in rats with experimentally induced epilepsy, CRF enhanced, rather than suppressed, neuronal activity in this part of the brain. In the brains of epileptic rodents, the receptor for CRF signaled through a different G α protein, and G protein switching contributed to the CRF-induced enhancement in neuronal activity. These results may explain why stress and anxiety tend to increase the frequency of seizures in epileptics.